ORGANOMETALLICS

Article

pubs.acs.org/Organometallics

Triazolylidene Iron(II) Piano-Stool Complexes: Synthesis and Catalytic Hydrosilylation of Carbonyl Compounds

Chloe Johnson and Martin Albrecht*

Departement für Chemie und Biochemie, Universität Bern, Freiestrasse 3, CH-3012 Bern, Switzerland

Supporting Information

ABSTRACT: A new series of iron(II) piano stool complexes was synthesized that contain monodentate triazolylidene ligands with different aryl and alkyl substituents as well as an example of a C,N-chelating pyridine-substituted triazolylidene iron complex. The electronic and steric effect of wingtip modification was assessed by electrochemical, infrared spectroscopic, and X-ray diffraction analysis. All complexes were active in the catalytic hydrosilylation of aldehydes and ketones. The monodentate systems outperform the chelating triazolylidene analogue by far, reaching turnover frequencies TOF_{max} as high as 14400 h^{-1} at 0.1 mol % catalyst loading. Mechanistic investigations indicate a radical mechanism for the catalytic H−Si bond activation.

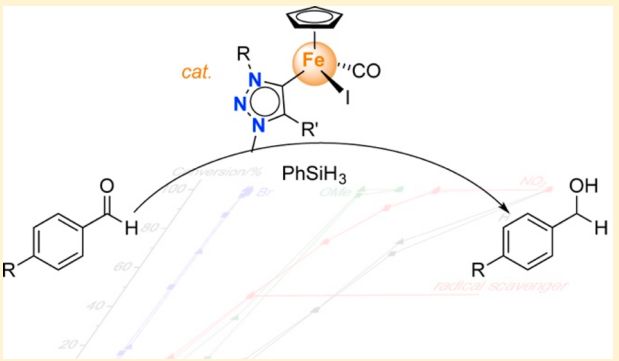

INTRODUCTION

Iron is inexpensive, earth-abundant, nontoxic, biologically relevant, and environmentally benign. Thus, iron catalysts offer an attractive alternative to systems based on rare and precious platinum-group and coinage metals which dominate the current literature.[1] In recent years, iron-catalyzed reduction of unsaturated compounds has become an active area of research, with advances in direct hydrogenation, transfer hydrogenation, and hydrosilylation catalysis.[2] Even though N-heterocyclic carbenes (NHCs) have made substantial contributions to almost all areas of catalysis,[3] only a few NHC iron complexes have been shown to catalyze such reduction reactions.[4] The first example of Fe-NHC-catalyzed hydrosilylation of carbonyl compounds was reported by Royo and coworkers.[5] Following this work, protocols have been developed toward the reduction of a wide range of functional groups, including carbonyl,[5,6] nitrile,[7] imine,[8] and sulfoxide moieties.[9] In contrast to direct and transfer hydrogenation, hydrosilylation catalysis can be operated under relatively mild conditions (base free, nonreducing environment), utilizing nontoxic silicon reagents, which makes this transformation a valuable methodology for the reduction of unsaturated organic compounds.[10]

1,2,3-Triazolylidenes are a recently developed subclass of NHC ligands[11] which have tremendous versatility due to the synthetic flexibility of the cycloaddition of alkynes with azides (CuAAC).[12] These ligands are strong σ donors, exhibiting stronger donor properties in comparison to classic Arduengo-type imidazol-2-ylidenes, yet weaker than "abnormal" imidazol-4-ylidenes.[13] This property, coupled with the electronic flexibility of the mesoionic ligands, makes them a powerful class of ligands for a large variety of catalytic transformations including olefin metathesis,[14] cross coupling,[15] and oxidation of water[16] and organic compounds.[17] To date, 1,2,3-triazolylidenes have been underexploited as ligands for first-row transition metals, with only a few examples in the literature.[15d,18] Building on our recent progress in using triazolylidene nickel complexes as efficient catalysts for the selective hydrosilylation of aldehydes,[19] we here report on the synthesis of monodentate 1,2,3-triazolylidene Fe(II) piano-stool complexes, with aryl and alkyl wingtip substituents as well as a chelating pyridyl unit. These complexes were screened for the catalytic hydrosilylation of aldehydes and ketones, and mechanistic aspects were investigated.

RESULTS AND DISCUSSION

Synthesis of Triazolylidene Fe^{II} Complexes. The triazolium salt ligand precursors **1** were accessed by the regioselective copper-catalyzed [2 + 3] cycloaddition of the relevant alkyne and azide,[12] followed by N3 methylation of the resulting 1,4-disubstituted 1,2,3-triazoles. Application of the established free carbene route using KO^{t}Bu as base[14a,20] and $[CpFe(CO)_2I]$ as metal precursor provided the cationic complexes **2a−d** and **5** (Scheme 1).

Due to the potential for methyl group rearrangement of the free carbene ligand after deprotonation,[14a,20a] a solution of the free carbene was typically added to the $[CpFe(CO)_2I]$ metal precursor after short reaction times of 15−20 min. While single crystals suitable for X-ray diffraction were obtained, the cationic complexes **2** proved challenging to purify in the bulk phase. Residual triazolium salt was constantly present, since all purification efforts resulted in partial decomposition of the complex in addition to the gradual formation of the neutral complexes **4**. The latter issue was circumvented by exchanging

Received: May 8, 2017

DOI: 10.1021/acs.organomet.7b00349
Organometallics XXXX, XXX, XXX−XXX

Scheme 1. Synthesis of Mondentate and Chelating Triazolylidene Fe(II) Complexes[a]

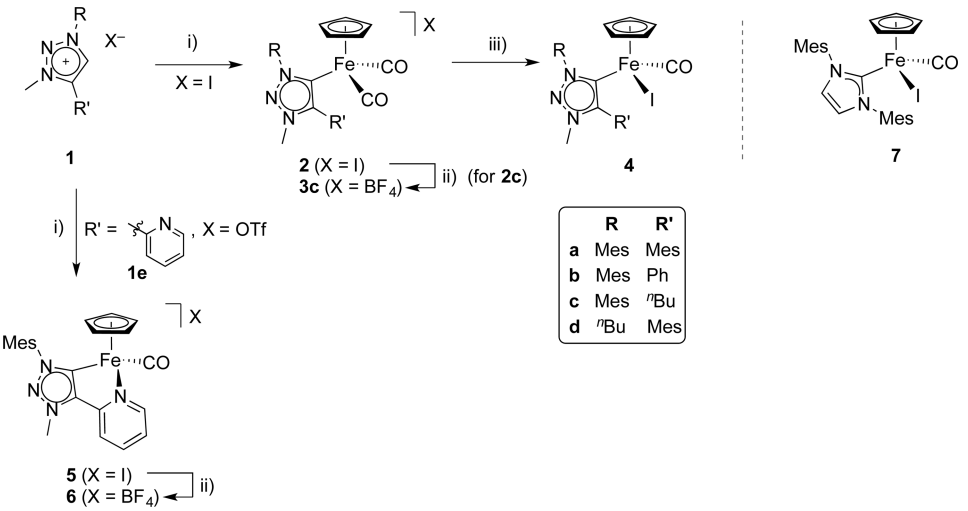

[a]Reagents and conditions: (i) KO^{t}Bu, THF, room temperature, 20 min followed by [CpFe(CO)$_2$I], toluene, room temperature, 20 h; (ii) AgBF$_4$, CH$_2$Cl$_2$, room temperature, 1 h; (iii) $h\nu$, CH$_2$Cl$_2$, 16 h.

the iodide counterion in **2** for BF_4^- (complexes **3**). In contrast, the neutral complexes **4** were isolated in acceptable yields after irradiation of the crude material, which induced the loss of one CO ligand and coordination of the iodide anion. This transformation was accompanied by a diagnostic color change of the solution from yellow to green. The pyridine-functionalized triazolium salt precursor gave exclusively the chelate product **5**, with no indication of a monodentate species present. All complexes are stable to air in the solid state, while in solution they decompose to a paramagnetic species within a few hours unless handled under an inert atmosphere.

The disappearance of the characteristic triazolium proton signal at δ_H 9.1 ± 0.7 in combination with the expected relative integration of the NCH$_3$ and Cp fragments in the ^{1}H NMR spectra supported the formation of the proposed cationic complexes **2** and **3**. The appearance of a signal at δ_C 152.3 ± 1.4 corresponding to the Fe−C$_{carbene}$ was further indication of successful complexation. The transformation to the more electron rich neutral complexes **4** was indicated by an upfield shift of the Cp carbon signals from δ_C 86.8 ± 0.1 to 80.1 ± 0.3. Concurrently, the Fe−C$_{carbene}$ resonances shifted markedly downfield to δ_C 173.5 ± 3.4.

IR Spectroscopic and Electrochemical Analyses. The infrared absorption bands corresponding to the carbonyl ligands were a useful probe for the conversion of cationic complexes **2** to the neutral analogues **4** (Table 1) and furthermore allowed determination of the relative basicity of the triazolylidene ligands. The cationic monocarbene complexes **2** and **3** (ν_s 2044 ± 3 cm^{-1}, ν_{as} 1998 ± 4 cm^{-1}) gave bands similar to those of the precursor complex [CpFe(CO)$_2$I] (ν_s 2041 cm^{-1}, ν_{as} 1997 cm^{-1}), suggesting that the donor properties of the triazolylidene ligands are similar to those of iodide. The trend of carbonyl stretching frequencies within the series of complexes **2a−d** and **3c** does not reflect the expected relative donor/acceptor influences of the wingtip substituents. For instance, the *N*-mesityl, *C*-phenyl substitution pattern of complex **2b** promotes increased π back-donation to the carbonyl ligands according to the pertinent IR frequencies (ν_s 2041 cm^{-1}, ν_{as} 1994 cm^{-1}) in comparison to the *N*,*C*-dimesityl-substituted NHC complex **2a** (ν_s 2047 cm^{-1}, ν_{as} 2002 cm^{-1}), despite the fact that the phenyl group is electron-poorer than the mesityl unit. With an alkyl donor substituent at the C4 position as in complexes **2c**/**3c**, lower CO stretching frequencies were observed (**2c**, ν_s 2040 cm^{-1}, ν_{as} 1993 cm^{-1}; **3c**, ν_s 2041 cm^{-1}, ν_{as} 1994 cm^{-1}) in comparison to the isomer containing the alkyl substituent on the N1 position (ν_s 2046 cm^{-1}, ν_{as} 1998 cm^{-1} in **2d**).

Table 1. Vibrational and Electrochemical Data for Cationic and Neutral Fe(II) Complexes

complex	N_{trz}-R	C_{trz}-R′	ν(CO)[a]	$E_{1/2}$ vs SCE[b]
2a	Mes	Mes	2047, 2002	
2b	Mes	Ph	2041, 1994	
2c	Mes	^{n}Bu	2040, 1993	
3c	Mes	^{n}Bu	2041, 1994	
2d	^{n}Bu	Mes	2046, 1998	
4a	Mes	Mes	1933	+0.34
4b	Mes	Ph	1935	+0.38
4c	Mes	^{n}Bu	1935	+0.38
4d	^{n}Bu	Mes	1937	+0.38
6	Mes	pyr	1971	+1.14
7[c]			1938	+0.41

[a]In cm^{-1}, measured in CH$_2$Cl$_2$. [b]In V vs SCE ($E_{1/2}$(Fc$^+$/Fc) at +0.46 V), measured in CH$_2$Cl$_2$, 0.1 M [Bu$_4$N][PF$_6$] electrolyte, sweep rate 250 mV s^{-1}. [c]From ref 20b, sweep rate 100 mV s^{-1}.

A single lower energy CO absorption band at 1935 ± 2 cm^{-1} emerges as the neutral monocarbonyl complexes **4** are formed. The almost identical vibrational frequencies observed for these complexes suggest that variation of the wingtip substituents has only a minor influence on the donor strength of the ligands. As for the dicarbonyl complexes, the CO stretching frequencies do not correlate with the intuitively assumed donor/acceptor influence of the wingtip substituents. Most striking is that complexes **4c**,**d** (ν 1935, 1937 cm^{-1}) with electron-donating *n*-butyl substitution have a higher energy CO vibration, typically attributed to poorer donor properties, in comparison to dimesityl complex **4a** (ν 1933 cm^{-1}) yet comparable to the frequency in complex **4b** with a *N*-mesityl, *C*-phenyl substitution pattern (ν 1935 cm^{-1}). We therefore assume that stereoelectronic effects affect the CO vibrational energies

DOI: 10.1021/acs.organomet.7b00349
Organometallics XXXX, XXX, XXX−XXX

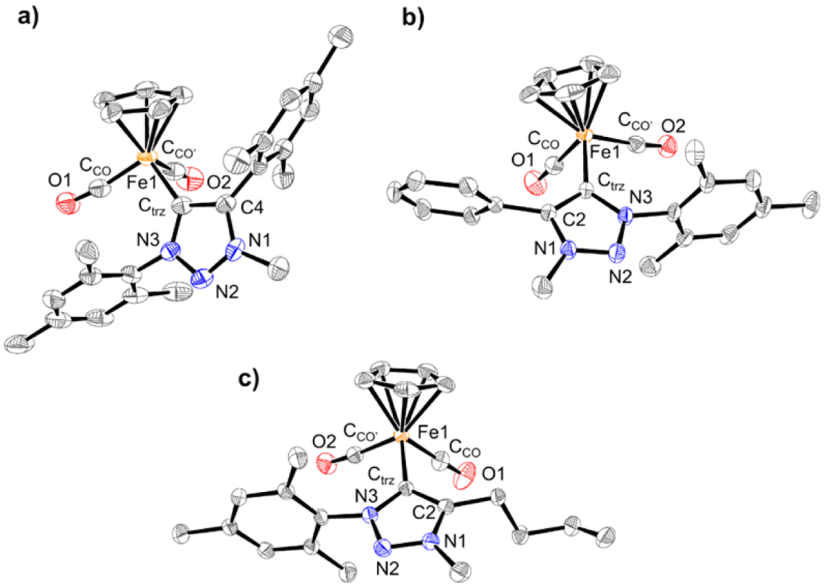

Figure 1. ORTEP representations of the cationic complexes (a) **2a**, (b) **2b**, and (c) **3c** (all 50% probability level; hydrogen atoms and noncoordinating anions omitted for clarity).

substantially more than the inductive electronic effects of the triazolylidene substituents.

Cyclic voltammetry data (Table 1) reinforce the marginal influence of wingtip substitution on the donor properties of the ligands. Accordingly, the bis(mesityl)-substituted triazolylidene in complex **4a** imparts more electron density to the iron(II) center ($E_{1/2}$ = +0.34 V vs. SCE) in comparison to alkyl-containing triazolylidene in complexes **4b,c** ($E_{1/2}$ = +0.38 V vs SCE). Therefore, the electronic contribution of the wingtip groups appears to be less important than stereoelectronic effects such as the arrangement of the carbene heterocycle with respect to the Fe orbitals.

IR and electrochemical comparison of triazolylidene and imidazolylidene ligands consistently indicate stronger donor properties for triazolylidenes, in good agreement with previous studies.[13d−f] For example, the CO vibration is lower in complex **4a** (ν 1933 cm^{-1}) than in the sterically analogous 2-imidazolylidene complex **7** (ν 1938 cm^{-1}). Cyclic voltammetric studies led to a similar conclusion, as iron(II) oxidation in the triazolylidene complex **4a** occurs at slightly lower potential ($E_{1/2}$ = +0.34 V) in comparison to the oxidation in the 2-imidazolylidene homologue **7** ($E_{1/2}$ = +0.41 V).

The appearance of just one carbonyl infrared band (ν 1971 cm^{-1}) for complex **5** confirmed the exclusive formation of the pyridine-carbene chelate complex. The band is significantly shifted to higher wavenumbers in comparison to the monodentate triazolylidene complexes **4**. These data coupled with the markedly higher oxidation potential (+1.14 V) of the iron center in **5** indicates a relatively electron deficient Fe(II) center, as expected when a cationic complex is compared with neutral analogues.

Solid-State Structures. The structures of the cationic complexes **2a,b** and **3c** were determined by X-ray crystallographic analysis (Figure 1). Selected bond lengths and angles are compiled in Table 2. The structures confirm the connectivity pattern surmised from solution analysis and reveal that the complexes adopt a piano-stool geometry. The Fe−$C_{carbene}$ bond distances (1.97−2.01 Å) are very similar to those in related imidazolylidene complexes[20b,c] and do not vary significantly within the monodentate series. The dihedral angle N3−C_{trz}−Fe1−$Cp_{centroid}$ in the dimesityl-functionalized complex **2a** is 139.91° and reveals a significant twist of the carbene heterocycle, while for the less bulky phenyl-mesityl-substituted triazolylidene complex **2b** the angle is appreciably smaller (110.90°). The least bulky *n*-butyl-mesityl ligand in **3c** induces the smallest angle of 98.38°. The variable orientation of the heterocycle with respect to the Fe−Cp vector presumably adjusts the degree of metal−ligand orbital overlap, which affects the donor properties of the carbene (cf. IR and CV data above). In particular, the twisted arrangement of **2a** and to a lesser extent **2b** may disrupt π back-donation to the carbene ligand and therefore increases the electron density at the metal center. Interruption of the π back-bonding in diaryl complex **2b** may account for its donor properties being similar to those of the more electron rich *N*-mesityl, *C*-*n*-butyl ligand in **3c**. A slightly longer Fe−$C_{carbene}$ bond length is noted for **2a** (2.010(6) Å) in comparison to **2b,c** (1.9745(18) and 1.9744(14) Å, respectively), which provides a potential rationale for the moderate donor properties of **2a**. Shorter C_{ipso}(N-mesityl)···CO distances are noted for the complexes with a greater degree of twist, e.g. ca. 2.91 Å in the most distorted complex **2a** in comparison to

Table 2. Selected Bond Lengths (Å) and Angles (deg) for Complexes 2a,b and 3c

	2a	2b	3c
Fe1−C_{trz}	2.010(6)	1.9745(18)	1.9744(14)
Fe1−C_{CO}	1.774(7)	1.764(2)	1.7670(16)
Fe1−$C_{CO'}$	1.767(6)	1.778(2)	1.7717(15)
Fe1−$Cp_{centroid}$	1.727	1.725	1.726
C_{CO}−O1	1.145(8)	1.140(3)	1.138(2)
$C_{CO'}$−O2	1.147(8)	1.138(3)	1.1412(18)
C_{CO}−Fe1−C_{trz}	99.0(3)	91.14(8)	90.26(7)
C_{CO}−Fe1−$C_{CO'}$	91.2(3)	93.06(10)	94.89(7)
$C_{CO'}$−Fe1−C_{trz}	90.7(3)	98.36(8)	97.54(6)
C_{trz}−Fe1−$Cp_{centroid}$	124.49	120.63	121.47
N3−C_{trz}−Fe1−$Cp_{centroid}$	139.91	110.90	98.38

DOI: 10.1021/acs.organomet.7b00349
Organometallics XXXX, XXX, XXX−XXX

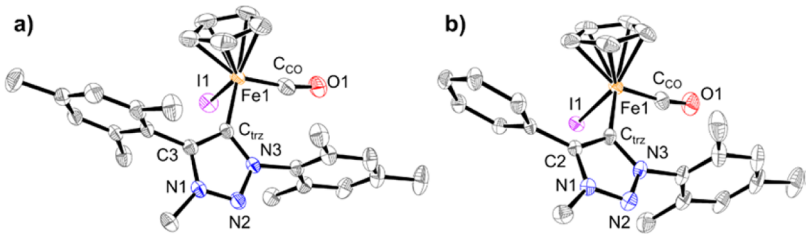

Figure 2. ORTEP representation (50% probability level) of the neutral complexes (a) **4a** and (b) **4b**. Hydrogen atoms have been omitted for clarity. The labeling of the nitrogen atoms in **4b** has been adjusted for consistency.

ca. 3.07 Å for complex **3c** ,in which the torsion angle N3−C_{trz}−Fe1−$Cp_{centroid}$ is much more acute (see Table S3 in the Supporting Information). The relatively short C_{ipso}···CO distances, coupled with a significant bending of the adjacent CO ligand away from the mesityl moiety (Fe−C−O ca. 170.5° for **2a**), is in agreement with an interligand $\pi(C_{ipso}{=}C){-}\pi^*(C{\equiv}O)$ interaction that may cause a slight red shifting of the ν(CO) frequency.[21]

The structures obtained for neutral complexes **4a,b** (Figure 2) confirm the successful exchange of one carbonyl ligand for an iodide. Fe−$C_{carbene}$ bond distances remain in the same range as for the dicarbonyl complexes (Table 3). The molecular

Table 3. Selected Bond Lengths (Å) and Angles (deg) for Complexes 4a,b

	4a	4b
Fe1−C_{trz}	1.974(3)	1.962(2)
Fe1−C_{CO}	1.747(3)	1.756(2)
Fe1−I1	2.6391(4)	2.6374(3)
Fe1−$Cp_{centroid}$	1.722	1.723
C_{CO}−O1	1.152(4)	1.148(3)
C_{CO}−Fe1−C_{trz}	99.48(13)	99.78(10)
C_{trz}−Fe1−I1	92.16(7)	91.96(6)
C_{CO}−Fe1−I1	89.91(10)	87.72(7)
C_{trz}−Fe1−$Cp_{centroid}$	125.15	122.83
N3−C_{trz}−Fe1−$Cp_{centroid}$	135.78	124.06

structure of **5** (Figure 3) unambiguously confirms the chelating *C,N*-bidentate bonding mode with a relatively strained bite angle of 80.28(15)°. The Fe−carbene bond (1.928(4) Å) is slightly shorter than the bond in the monodentate carbene

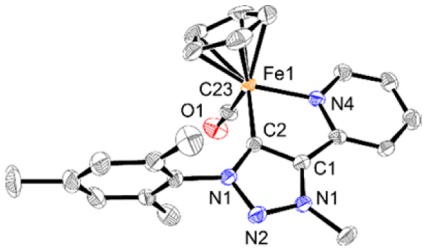

Figure 3. ORTEP representation (50% probability level) of the pyridine chelate complex **5**. Hydrogen atoms, a noncoordinating iodide, and cocrystallized CH_2Cl_2 solvent molecule have been omitted for clarity. Selected bond lengths (Å) and bond angles (deg): Fe1−C2 1.928(4), Fe1−C23 1.757(4), Fe1−N4 2.008(3), Fe1−$Cp_{centroid}$ 1.714, C23−O23 1.144(5); C23−Fe1−C2 95.31(17), C2−Fe1−N4 80.28(15), C23−Fe1−N4 96.09(17).

complexes and is in good agreement with those for related complexes with chelating picolyl-substituted imidazolylidene ligands.[20c] Similar to the case for the cationic complex **2a**, dimesityl complex **4a** has a larger N3−C_{trz}−Fe1−$Cp_{centroid}$ torsion angle of 135.78° in comparison to **4b** bearing a less bulky mesityl-phenyl substitution (124.06°). Again, the more twisted orientation of the triazolylidene ligand in **4a** may account for the increased electron density at the Fe center in comparison to **4b**. Furthermore, as discussed above for the cationic complexes, the slightly shorter C_{ipso}···CO distance in **4a** vs **4b** (ca. 2.90 vs 2.93 Å) may contribute to greater interligand π donation and thus a lengthening of the CO bond.

Catalytic Hydrosilylation of Carbonyl Compounds. On the basis of the recent success of analogous imidazolylidene and imidazolinylidene iron piano-stool complexes in the reduction of carbonyl compounds,[5,6] we screened the activities of all complexes for catalytic hydrosilylation using 4-nitrobenzaldehyde as a model substrate and phenylsilane in 1,2-dichloroethane.[15d] The known IMes piano-stool complex **7**[20b] and the [$CpFe(CO)_2I$] precursor were also tested under the same conditions. The conversion of the aldehyde substrate to a mixture of silylated products at 60 °C was monitored over time (Figure 4), and selected conversions are presented in Table 4.

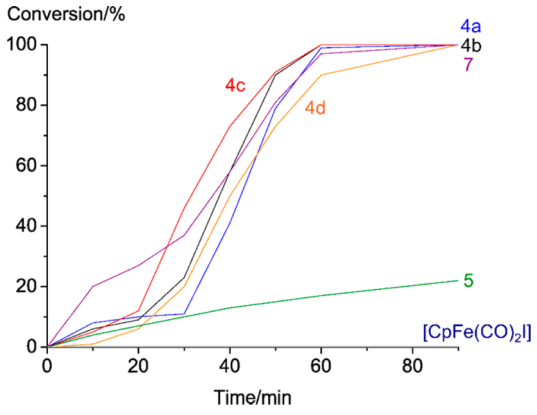

Figure 4. Time-dependent conversion of 4-nitrobenzaldehyde in 1,2-dichloroethane catalyzed by iron(II) complexes.

Due to considerable spectral overlap, it was difficult to unambiguously characterize the identity and ratio of silyl ether products. Therefore, the conversion of the aldehyde was determined with respect to hexamethylbenzene as internal standard. At relatively low catalyst loadings of 1 mol %, complexes **4a,b** achieve full conversion after 1 h (entries 1 and 2), while the aldehyde is between 90 and 99% converted when using complexes **4c,d** and **7** (entries 3, 4, and 6). A time−conversion profile (Figure 4) evidences only minor variation in the activity upon changing the wingtip substituents within the

DOI: 10.1021/acs.organomet.7b00349
Organometallics XXXX, XXX, XXX−XXX

Table 4. Conversion of 4-Nitrobenzaldehyde at Selected Time Points Catalyzed by Iron(II) Complexes[a]

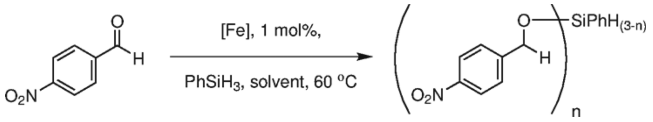

entry	complex	solvent	conversion (%)[b]	TOF_{max} (h^{-1})	approx induction time (min)
1	**4a**	DCE	99	230	30
2	**4b**	DCE	100	210	20
3	**4c**	DCE	100	200	20
4	**4d**	DCE	90	180	20
5	**5**	DCE	17	20	
6	**7**	DCE	97	140	30
7	$[CpFe(CO)_2I]$	DCE	0		
8	**4c**	THF	98	190	0
9	**4c**	DCB	71	120	10
10	**4c**	toluene	51	130	10
11[c]	**4c**	DCE	9		
12		THF	5		
13		DCE	0		

[a]General conditions: 4-nitrobenzaldehyde (0.5 mmol), phenylsilane (0.6 mmol), [Fe] precatalyst (1 mol %; 5 μmol), C_6Me_6 (50 μmol), and solvent (2.5 mL). [b]Conversion determined at 1 h by ^1H NMR spectroscopy using C_6Me_6 as internal standard and calculated as an average of two or more runs. [c]Reaction carried out at 30 °C. Conversion determined at 24 h.

triazolylidene monodentate series. All complexes have an induction period of about 20−30 min where activity is low (initial turnover frequency, $TOF_{initial}$ = 30 ± 10 h^{-1}), followed by a burst in activity where the conversion is essentially complete within a further 30 min (maximum turnover frequency, TOF_{max}[22] around 200 ± 30 h^{-1}). The initial TOF is much faster for the 2-imidazolylidene complex **7** ($TOF_{initial}$ = 120 h^{-1}, entry 6); however, the maximum TOF (140 h^{-1}) does not reach that of triazolylidene complexes **4a−d** (entries 1−4). The addition of the pyridine moiety in complex **5** has a detrimental effect and significantly lowers the activity (TOF_{max} = 20 h^{-1}), affording only 17% conversion after 60 min (entry 5). In comparison and as a reference, the iron(II) precursor $[CpFe(CO)_2I]$ shows no conversion of substrate under the applied conditions (entry 7), underpinning that the triazolylidene ligand is critical for promoting catalytic activity.

Because of its fast conversion and relatively short induction time, complex **4c** was selected to optimize the hydrosilylation of 4-nitrobenzaldehyde with phenylsilane (Table 4, entries 3 and 8−11; see Figure S24 in the Supporting Information). DCE and THF (entries 3 and 8) emerged as the most suitable solvents, with conversions of 98 and 100%, respectively, after 1 h. Only a moderate conversion of 71% was reached after the same time using an alternative chlorinated solvent, 1,2-dichlorobenzene (DCB, entry 9). Similarly, toluene (entry 10, 51% conversion after 1 h) was a comparatively poor solvent for the reaction. As for DCE, induction times were observed when DCB and toluene were selected as solvents. Initial TOFs resembled those for DCE; however, maximum TOFs were lower (130 and 120 h^{-1}). In contrast, 4-nitrobenzaldehyde was converted without any induction time in THF with a TOF_{max} value of 190 h^{-1}. Heating is required for the reaction to occur in DCE, as evidenced by the negligible conversion of 9% obtained after 24 h at 30 °C (entry 11). The role of **4c** as precatalyst for the hydrosilylation reaction was further confirmed by carrying out blank reactions in THF and DCE (entries 12 and 13) at 60 °C. In particular, is it clear that a catalyst is required in DCE solvent, as the blank reaction revealed zero conversion after 1 h. Conversely, in THF, a small amount of aldehyde substrate (5% after 1 h) is converted in the absence of catalyst.

Further screening of aldehyde substrates with substituents para to the carbonyl moiety (Table 5) was carried out with **4c** as precatalyst in order to determine the tolerance of the reaction to these functional groups and moreover to probe the dependence of the reaction rate on the substituent Hammett parameters. All aldehyde substrates were converted within 60 min, with nitro, bromo, nitrile, dimethylamino, trifluoromethane, and methoxy substituents being tolerated (entries

Table 5. Conversion of Aldehydes and Ketones Catalyzed by Complex 4c[a]

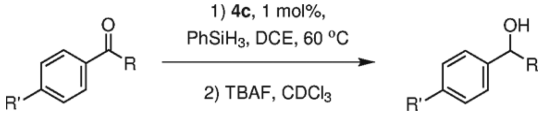

entry	R	R′	time (min)	conversn (%)[b]	yield (%)[c]	σ_p[d]	induction time (min)	TOF_{max} (h^{-1})
1	H	NO_2	60	100	89	0.71	20	200
2		CN	10	100	99	0.66	4	1140
3		CF_3	30	100	100	0.54	18	870
4		Br	9	100	100	0.23	5	2580
5		H	20	100	98	0	14	1890
6		CH_3	50	98	100	−0.17	25	410
7		OMe	50	100	100	−0.27	20	450
8		NMe_2	18	100	90	−0.87	10	1560
9	CH_3	Br	60	97	96	0.23		
10		H	120	98	98	0		
11		OMe	150	98	97	−0.27		

[a]General conditions: substrate (0.5 mmol), phenylsilane (0.6 mmol), [Fe] precatalyst (1 mol %; 5 μmol), C_6Me_6 (50 μmol) and 1,2-DCE (2.5 mL). [b]Conversion determined by ^1H NMR using C_6Me_6 as internal standard. [c]Spectroscopic (^1H NMR) yield of alcohol product after silyl deprotection. [d]From ref 24.

DOI: 10.1021/acs.organomet.7b00349
Organometallics XXXX, XXX, XXX−XXX

1−8). No reduction of the nitro or nitrile groups or dehalogenation was observed. Since multiple silylated products can potentially be obtained, the spectroscopic yield was determined following fluoride-mediated cleavage of the O−Si bond to give exclusively the alcohol product. These yields were consistently very good to excellent, ranging between 89 and >99%. Analysis of the time-dependent conversion profile of the benzaldehyde derivatives reveals that all substrates are converted with distinct induction periods (Figure 5). Induction

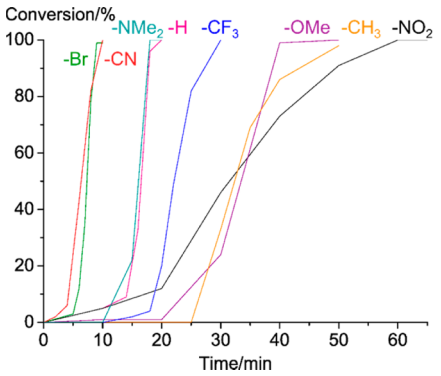

Figure 5. Time-dependent conversion of para-substituted benzaldehydes catalyzed by **4c** in DCE. Para substituents are indicated in the figure.

times range between 4 and 25 min, with no apparent correlation between classic Hammett parameters for the substitutions and the length of the induction time or the conversion rate. However, we note that the induction period is reproducible, suggesting a programmed activation rather than an uncontrolled decomposition.[23]

When the hydrosilylation of 4-nitrobenzaldehyde was run in THF rather than in DCE, the time-dependent conversion profile revealed no induction time. It was therefore interesting to see if THF induces a different mechanism. To probe this hypothesis, catalytic runs of the various aldehydes were carried out in both solvents (Table 5 and Table S4 in the Supporting Information). The time-dependent conversion shows similar features, irrespective of the solvent used. The induction time is only absent when 4-nitrobenzaldehyde or 4-cyanobenzaldehyde was used as substrate, though all other substrates show an induction time, which is typically slightly shorter in THF in comparison to reactions in DCE. However, the TOF_{max} values for the majority of the substrates do not vary significantly upon changing the solvent, nor do the times required for full conversion. An exception is 4-cyanobenzaldehyde, which is converted at a far higher TOF_{max} value of 2070 h^{-1} in THF in comparison to 1240 h^{-1} in DCE. The conversion of 4-dimethylaminobenzaldehyde also features a solvent dependence, with DCE promoting much faster rates (TOF_{max} = 1560 h^{-1}) vs THF (TOF_{max} = 500 h^{-1}). Conversions are consistently high (≥98%) in both THF and DCE. The largely similar reaction profiles in both THF and DCE, and most notably the presence of an induction time in both cases, suggest that the mechanism is not solvent dependent. In particular, we have shown that 1,2-dichloroethane, a potential oxidant, is not the cause of the induction time.

When the loading of complex **4c** was decreased for the conversion of 4-bromobenzaldehyde at constant substrate concentration in DCE, the induction time increased. For example, lowering the catalyst ratio from 1.0 to 0.3 mol % doubled the induction time from ca. 6 to 12 min (Figure 6). The TOF_{max} value, however, increases because of the higher

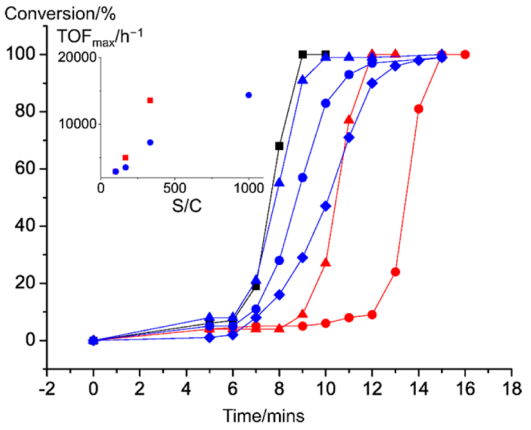

Figure 6. Time-dependent conversion of 4-bromobenzaldehyde catalyzed by **4c** in DCE: (black line) standard conditions using 2 mM [Fe] and 0.20 M aldehyde (S:C 100:1); (blue lines) [Fe] concentration kept constant (2 mM) and variation of the aldehyde concentration to 0.33 M aldehyde (triangles, S:C 167:1), 0.67 M aldehyde (circles, S:C 333:1), and 2.0 M aldehyde (diamonds, S:C 1000:1); (red lines) aldehyde concentration kept constant (0.20 M) and variation of the [Fe] concentration to 1.2 mM [Fe] (triangles, S:C 166:1), and 0.6 mM (circles, S:C 333:1). Inset: plot of S:C vs TOF_{max} upon varying the aldehyde concentration (blue) and the catalyst concentration (red).

substrate to catalyst ratio (S:C). Remarkably, further lowering of the catalyst loading to 0.1 mol % (0.2 mM in **4c**) is too low to achieve substrate conversion. If, however, the catalyst concentration is kept constant (2.0 mM) and the substrate concentration is increased, leading to the same 1000:1 S:C ratio, conversion is essentially quantitative within 15 min and the catalyst reaches a TOF_{max} value of 14400 h^{-1}. Attempts to increase the S:C ratio to 10000:1 by a further increase of the substrate concentration (19.8 M; 12.5 mmol of 4-bromobenzaldehyde in 0.63 mL of DCE) resulted in only 40% conversion after 25 h, corresponding to 4000 catalytic turnovers, which presumably represents the limits of the active catalyst before gradual deactivation occurs. Furthermore, the very high substrate concentrations may alter the solvation properties substantially, which may suppress high catalytic activity, preventing full aldehyde conversion. Adjusting the S:C ratio to 333:1 by decreasing the concentration of the iron complex increased the induction time; however, it gave a significantly higher TOF_{max} (approximately 13600 h^{-1}) in comparison to that upon an increase in the substrate concentration to achieve the same S:C ratio (TOF_{max} = 7300 h^{-1}; Figure 6, inset).

Ketone reduction was probed using para-substituted acetophenones in DCE solvent (cf. Table 5). Excellent yields were accomplished; however, reaction times were longer than with aldehydes and up to 250 min was required to reach high conversions. Using these reaction conditions, the activity surpasses that observed for analogous imidazolylidene,[6d] imidazolinylidene,[6a] and benzimidazolylidene[6] complexes, which typically need longer reaction times. However, the activity is not as high as for a related NHC-iron piano-stool hydroxide complex.[6e] Motivated by the considerably slower reactivity of ketones in comparison to aldehydes, we investigated whether aldehydes can be preferentially converted in the presence of ketones by rigidly controlling reaction times.

DOI: 10.1021/acs.organomet.7b00349
Organometallics XXXX, XXX, XXX−XXX

To probe such selectivity aspects, a 1:1 mixture of 4-bromobenzaldehyde and 4-acetophenone was used as a substrate mixture. Interestingly, a significant increase in the rate of ketone conversion was observed (92% in 10 min vs 50 min in the absence of aldehyde; Figure 7). We tentatively

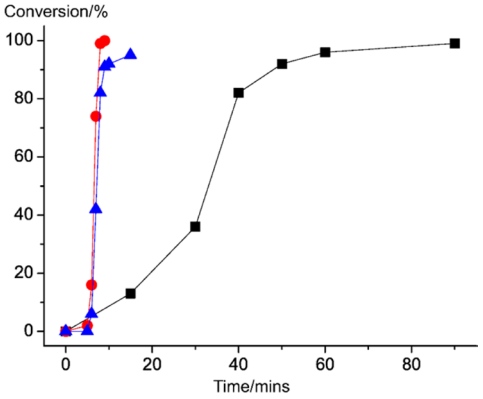

Figure 7. Time-dependent conversion of 4-bromoacetophenone (0.2 M) in the presence (blue triangles) and absence (black squares) of 4-bromobenzaldehyde (0.2 M; conversion represented by red circles) catalyzed by **4c** (2 mM) under standard conditions (cf. Table 4).

attribute this behavior to the accelerated formation of the catalytically active species in the presence of 4-bromobenzaldehyde, which then converts both ketones and aldehydes at high rates.[25] Alternatively an autocatalytic mechanism may be operating, whereby a product of the catalytic reaction increases the turnover frequency. To address the first possibility, the catalyst was prestirred with the aldehyde substrate for the length of the induction time before addition of the silane. The induction period of this run was identical with that under the standard conditions (see Figure 5), which indicates that the catalyst activation is not triggered by (slow) adduct formation between the iron complex and the aldehyde substrate.

Since recent studies have suggested that Fe−$C_{carbene}$ bonds are weaker than those formed between carbenes and platinum-group metals,[26] we sought to investigate if free carbene was released during the catalysis, a process that might lead to an organocatalytic cycle with the free carbene as the true catalytically active species. Relevant in this context, the nucleophilicity of free NHCs has been exploited for organocatalysis, including the catalytic hydrosilylation of CO_2, ketones, and imines.[27] In a control experiment, we succeeded in trapping freshly prepared IMes by S_8 within seconds, and a sample collected after 15 s contained the corresponding thiourea exclusively.[28] This experiment indicates that trapping of the free carbene is quasi-instantaneous and that the thiourea product is a suitable probe for the formation of free NHC. When S_8 (5 mol %) was introduced at the beginning of the catalytic reaction using 4-bromobenzaldehyde as substrate and complex **7** as precatalyst, the reaction was severely inhibited, with conversions achieving only 25% after 9 min (cf. full conversion in the absence of sulfur). When S_8 was introduced shortly after the induction period (t = 3 min, 28% conversion), the catalytic reaction immediately ceased with no further conversion detected after sulfur addition. In order to determine if this inhibition was due to trapping of catalytically active free NHC by sulfur, the IMes complex **7** was exposed to an excess of S_8. After 10 min (1,2-dichlorobenezene at 60 °C), i.e. the time period relevant to catalysis and required for complete conversion of 4-bromobenzaldehyde, a sample was taken and diluted with C_6D_6. According to the resulting ^{1}H NMR spectrum, the complex is robust within this period, with no indication of thiourea formation within the detection limits of the NMR measurement.[29] Therefore, it seems unlikely that significant levels of potentially catalytically active free carbene are present within the time frame of the reaction. The observed catalyst inhibition may instead be related to the formation of strong Fe−S bonds which poison the catalyst.

Classically, hydrosilylation is assumed to involve a metal hydride species, into which the carbonyl group inserts.[30] For the triazolylidene iron species investigated here, however, several features of the catalysis point toward a radical-based catalytic reaction mechanism. The induction time, for instance, may correspond to an initiation step which generates free radicals, which once formed accelerate the rate of reaction. Likewise, the absence of any Hammett correlation and the specific concentration dependence lend support to a radical mechanism. Furthermore, the marked enhancement of the rate of 4-bromoacetophenone conversion in the presence of 4-bromobenzaldehyde can be rationalized by faster initiation by the aldehyde. We speculate that a persistent Fe(II) radical species is formed[31] either from homolytic cleavage of a Fe^{III}−H species from hydrosilylation of the Fe−X bond[32] or from homolytic cleavage of an Fe^{III}−$O_{alkoxide}$ species which can then further react with the silane to yield the product (Scheme S1 in the Supporting Information). Such a persistent radical mechanism is supported by the noted enhancement of TOF_{max} upon diluting the concentration of Fe at a given S:C ratio (e.g., 333:1; cf. the inset in Figure 6). Lower concentrations of Fe reduce the potential for radical pairing as a catalyst deactivation pathway. Furthermore, a complex with a higher $Fe^{II/III}$ oxidation potential such as the pyridine-chelate complex **5** or [$CpFe(CO)_2I$] have significantly lower or even negligible catalytic activity, respectively. When the pronounced influence of the carbonyl substrate on the reaction rates is considered, it is plausible that Fe^{III}−O rather than Fe^{III}−H systems form the

Scheme 2. Inhibited Conversion of 4-Bromobenzaldehyde Catalyzed by 4c or 7 in the Presence of Additives

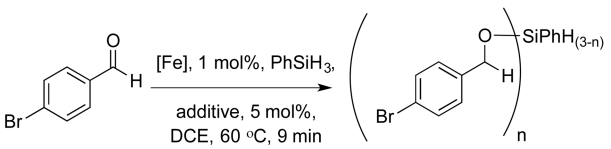

complex	additive	conversion/%
4c	-	100
7	-	100
7	S_8	25
4c	TEMPO	9
4c	BHT	15

DOI: 10.1021/acs.organomet.7b00349
Organometallics XXXX, XXX, XXX−XXX

Scheme 3. Expected Products without (Route A) and with (Route B) a SET-Induced Ketyl Radical Anion Intermediate[a]

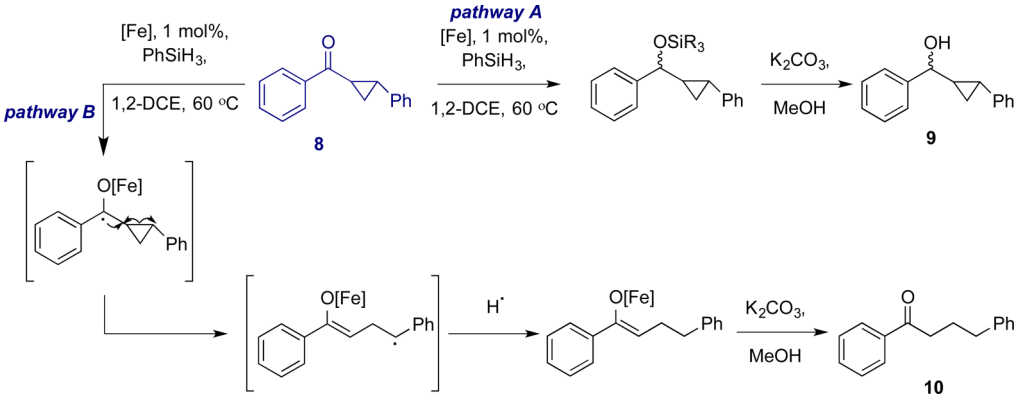

[a]The scheme is adapted from ref 30d.

persistent Fe radical as the active species for catalytic Si−O bond formation. Such a model is also corroborated by the different rates for aldehydes and ketones, as obviously the alkoxy radical is more stabilized in secondary than in primary alkoxy species.[33]

Prompted by these observations and the high propensity for iron to participate in single electron transfer (SET) processes,[1b,34] we investigated the influence of radical traps on the catalytic activity. When catalytic reactions were performed with the radical spin traps 2,2,6,6-tetramethylpiperidine *N*-oxide (TEMPO) or butylated hydroxytoluene (BHT), catalytic conversions were substantially inhibited. Hydrosilylation of 4-bromobenzaldehyde using catalyst precursor **4c** (1 mol %) in the presence of 5 mol % of the relevant scavenger afforded only 15% and 9% conversion for BHT and TEMPO, respectively (Scheme 2). These results are in agreement with the presence of radical species as catalytic intermediates which are deactivated by radical scavengers.

Further mechanistic investigations included the use of a radical clock, as such probes have previously been employed as useful indicators for a radical mechanism in iron-catalyzed cross-coupling reactions.[35] For our purposes, the radical clock **8**[36] was selected, which was comprised of a cyclopropyl unit incorporated into the α position of the ketone substrate (Scheme 3). Cyclopropyl ring opening by a potentially formed ketyl radical is known to occur quickly ($k_{obs} = 9 \times 10^5$ s^{-1} at 61 °C),[37] followed by hydrogen atom abstraction and formation of an enolate intermediate, which tautomerizes to the corresponding ketone in the presence of a base (Scheme 3, pathway B).[30d] When a catalytic run was performed with complex **4c** as precatalyst and radical clock **8** as substrate (S:C 100:1), only the alcohol product **9** derived from hydrosilylation and desilylation was observed after exposure to methanolic base (pathway A). Even though a SET process from the iron(II) center is principally plausible to generate a ketyl radical as a catalytic intermediate, this radical clock experiment indicates that the ketyl radical is either not formed or is too short-lived to induce the formation of the ring-opened product. The latter model is consistent with a dormant formal iron(III) species and a persistent iron(II) radical which captures the radical more efficiently than the cyclopropane unit. Such a mechanism provides an alternative to the Fe^{I}/Fe^{III} mechanism discussed for iron-catalyzed bond activation,[38] and it is fundamentally different from classical hydrosilylation mechanisms proposed for platinum-group metals, which involve either 2e$^-$ oxidative addition/reductive elimination sequences or heterolytic bond cleavage mechanisms.[39]

CONCLUSION

A new series of 1,2,3-triazolylidene iron(II) piano-stool complexes has been prepared, including monodentate and C,N-chelating carbene complexes. The electronic and structural features of these complexes are only marginally affected by the wingtip substitution pattern (alkyl or aryl). The iron(II) complexes are active catalyst precursors for the hydrosilylation of aldehydes and ketones under relatively mild conditions, achieving excellent yields of alcohol product and hence providing an inexpensive alternative to platinum-group catalysts often used for this transformation. Within the monodentate triazolylidene iron series activities are very similar, again emphasizing the limited influence of the wingtip groups. Incorporation of a chelating pyridine moiety in the C4 position, however, significantly decreases catalytic performance. Even at relatively low catalyst loadings of 0.1 mol %, the catalyst maintains high activity and reaches TOF_{max} values as high as 14400 h^{-1}. Aldehydes are generally converted more quickly than ketone substrates. Interestingly, in mixed aldehyde/ketone reactions, the conversion of the ketone was accelerated significantly. While insights into the catalytic mechanism strongly support the formation of persistent radicals and a single electron transfer process, further work is currently in progress to better understand the significance of this acceleration and the observed induction time. In addition, further unsaturated functional groups are currently being screened to establish the scope and selectivity of the reaction.

EXPERIMENTAL SECTION

General Comments. Metalation reactions and purification of complexes were carried out under an inert nitrogen atmosphere using standard Schlenk techniques. Toluene, THF, CH_2Cl_2, Et_2O, and hexane were dried by passage through solvent purification columns. 1,2-Dichloroethane was dried over 4 Å molecular sieves and degassed with argon. Benzaldehyde was freshly distilled before use. All other reagents were commercially available and used without further purification. The synthesis of triazolium salts **1a**,**b**,**d**, complex **7**, mesityl azide, and 1-mesityl-4-(2-pyridyl)-1,2,3-triazole have been reported elsewhere.[15c,17d,20b,40] NMR spectra were measured at 25 °C on Bruker spectrometers operating at 300 or 400 MHz (^{1}H NMR) and 75 or 101 MHz (^{13}C{^{1}H} NMR), respectively. Chemical shifts (δ in ppm, coupling constants J in Hz) were referenced to residual solvent resonances downfield to $SiMe_4$. Assignments were made on

DOI: 10.1021/acs.organomet.7b00349
Organometallics XXXX, XXX, XXX−XXX

the basis of homo- and heteronuclear shift correlation spectroscopy. IR spectra were recorded on a Jasco 4700 FT-IR instrument in CH_2Cl_2 solution at 1 cm^{-1} resolution. Elemental analyses and ESI mass spectra were performed by the Mass Spectrometry Group at Universität Bern. UV irradiation was carried out using a UVP Blak-Ray B-100AP lamp. Cyclic voltammetry measurements were carried out using a Metrohm Autolab Model PGSTAT101 potentiostat employing a gastight three-electrode cell under an argon atmosphere. A platinum disk with 7.0 mm^2 surface area was used as the working electrode and polished before each measurement. The reference electrode was Ag/AgCl; the counter electrode was Pt foil. Bu_4NPF_6 (0.1 M) in dry CH_2Cl_2 was used as supporting electrolyte with analyte concentrations of approximately 1 mM. The ferrocenium/ferrocene (Fc^+/Fc) redox couple was used as an internal reference ($E_{1/2}$ = 0.46 V vs SCE).[41]

Synthesis of 1-Mesityl-4-(*n*-butyl)-1,2,3-triazole. Mesityl azide (725 mg; 4.50 mmol), 1-hexyne (0.57 mL; 4.95 mmol), $CuSO_4 \cdot 5H_2O$ (22 mg; 0.09 mmol) and sodium ascorbate (178 mg; 0.90 mmol) were suspended in a 1/1 v/v THF/H_2O solvent mixture (18 mL). The reaction mixture was irradiated for 6 h at 100 °C in the microwave. After this time, THF was removed in vacuo and the product extracted with CH_2Cl_2 (30 mL) and washed with dilute NH_4OH solution (3 × 10 mL), then H_2O (15 mL), and finally brine (10 mL). The solution was dried over Na_2SO_4, and all volatiles were removed to yield the triazole as a pale yellow oil (1.01 g; 92%). ^{1}H NMR ($CDCl_3$, 400 MHz): δ 7.31 (s, 1H, H_{trz}), 6.96 (s, 2H, H_{Mes}), 2.81 (t, J = 7.6 Hz, 2H, CH_2-C_{trz}), 2.33, 1.94 (2 × s, 9H, CH_3-C_{Mes}), 1.77−1.67 (m, 2H, CH_2-CH_2C_{trz}), 1.47−1.36 (m, 2H, CH_2-CH_3), 0.95 (t, J = 7.4 Hz, 3H, CH_3-CH_2). $^{13}C\{^1H\}$ NMR ($CDCl_3$; 101 MHz): δ 148.3 (C_{trz}−^{n}Bu), 139.8, 135.2 (2 × C_{Mes}-CH_3), 133.9 (C_{Mes}−N), 129.1 (C_{Mes}−H), 122.6 (C_{trz}−H), 31.7 (CH_2-CH_2C_{trz}), 25.5 (CH_2-C_{trz}), 22.4 (CH_2-CH_3), 21.2, 17.3 (2 × CH_3-C_{Mes}), 14.0 (CH_3-CH_2). HR-MS (ESI): calcd for $C_{15}H_{22}N_3$ $[M + H]^+$ m/z 244.1808, found m/z 244.1805. Anal. Found (calcd) for $C_{15}H_{21}N_3$ (243.35): C, 74.33 (74.03); H, 9.23 (8.70); N, 17.62 (17.27).

Synthesis of 1c. 1-Mesityl-4-(*n*-butyl)-1,2,3-triazole (1.01 g; 4.13 mmol) was dissolved in CH_3CN (17 mL) and MeI (2.57 mL; 41.30 mmol) added. The mixture was stirred at 100 °C under microwave irradiation for 6 h. All volatiles were removed, the residue was dissolved in minimum CH_2Cl_2, and the product was precipitated with Et_2O. The precipitate was collected and washed with Et_2O (2 × 5 mL). After it was dried overnight in vacuo, the product was obtained as an off-white solid (1.43 mg; 90%). ^{1}H NMR ($CDCl_3$, 400 MHz): δ 8.51 (s, 1H, H_{trz}), 7.01 (s, 2H, H_{Mes}), 4.50 (s, 3H, NCH_3), 2.81 (t, J = 8.0 Hz, 2H, CH_2-C_{trz}), 2.34, 2.09 (2 × s, 9H, CH_3-C_{Mes}), 1.89−1.76 (m, 2H, CH_2-CH_2C_{trz}), 1.55−1.42 (m, 2H, CH_2-CH_3), 0.97 (t, J = 7.4 Hz, 3H, CH_3-CH_2). $^{13}C\{^1H\}$ NMR ($CDCl_3$; 101 MHz): δ 146.4 (C_{trz}−^{n}Bu), 142.6, 134.5 (2 × C_{Mes}-CH_3), 131.3 (C_{Mes}−N), 130.3 (C_{trz}−H), 129.9 (C_{Mes}−H), 40.0 (NCH_3), 29.2 (CH_2-CH_2C_{trz}), 24.5 (CH_2-C_{trz}), 22.3 (CH_2-CH_3), 21.3, 18.1 (2 × CH_3-C_{Mes}), 13.8 (CH_3-CH_2). HR-MS (ESI): calcd for $C_{16}H_{24}N_3$ $[M - I]^+$ m/z 258.1965, found m/z 258.1962. Anal. Found (calcd) for $C_{16}H_{24}FeIN_3$ (385.29): C, 49.99 (49.88); H, 6.04 (6.28); N, 11.06 (10.91).

Synthesis of 1e. 1-Mesityl-4-(2-pyridyl)-1,2,3-triazole (2.60 g; 9.82 mmol) was dissolved in a 1/5 v/v CH_2Cl_2/Et_2O mixture (60 mL), the solution cooled to 0 °C, and MeOTf (1.20 mL; 10.80 mmol) added. After 30 min of stirring at 0 °C, further Et_2O (40 mL) was added and the resulting precipitate collected by filtration. The pure product was obtained by SiO_2 column chromatography using 1/2 v/v CH_3CN/CH_2Cl_2 as eluent (1.17 g; 28%). ^{1}H NMR ($CDCl_3$, 400 MHz): δ 9.52 (s, 1H, H_{trz}), 8.82−8.73 (m, 1H, H_{py}), 8.50 (d, J = 8.0 Hz, 1H, H_{py}), 8.07−7.98 (m, 1H, H_{py}), 7.55−7.48 (m, 1H, H_{py}), 7.08 (s, 2H, H_{Mes}), 4.81 (s, 3H, NCH_3), 2.39, 2.13 (2 × s, 6H, CH_3-C_{Mes}). $^{13}C\{^1H\}$ NMR ($CDCl_3$; 101 MHz): δ 149.8 (C_{pyr}−H), 142.9 (C_{Mes}-CH_3), 142.7 (C_{pyr}), 141.8 (C_{trz}-pyr), 138.9 (C_{pyr}−H), 134.4 (C_{Mes}-CH_3), 132.3 (C_{trz}-H), 131.3 (C_{Mes}-N), 130.1 (C_{Mes}-H), 126.6, 126.3 (2 × C_{pyr}-H), 42.0 (NCH_3), 21.4, 17.5 (2 × CH_3-C_{Mes}). HR-MS (ESI): calcd for $C_{17}H_{19}N_4$ $[M - OTf]^+$ m/z 279.1604, found m/z 279.1599. Anal. Found (calcd) for $C_{18}H_{19}F_3N_4O_3S$ (428.43): C, 50.19 (50.46); H, 4.63 (4.47); N, 13.43 (13.08).

General Procedure for the Preparation of Complexes 2−5. The triazolium salt (1 equiv) and KO*t*Bu (1.2 equiv) were suspended in dry THF (ca. 1 mL per 0.1 mmol). After 20 min of stirring at room temperature, the solution was filtered into a dry toluene (ca. 3 mL per 0.1 mmol) solution of $[CpFe(CO)_2I]$ (0.9 equiv). The resulting mixture was stirred at room temperature for 16 h. The precipitate was collected by filtration, washed with toluene (2 × 2 mL), extracted with CH_2Cl_2, and dried in vacuo to yield the crude product. Further purification was precluded by the ready transformation of complexes **2**−**4** in the presence of light and the tendency for ligand dissociation during manipulations.

*Synthesis of **2b**.* The complex was prepared from **1b** (220 mg; 0.54 mmol), KO*t*Bu (74 mg; 0.66 mmol), and $[CpFe(CO)_2I]$ (150 mg; 0.49 mmol). The crude product was obtained as a yellow powder (136 mg; 48%). Single crystals suitable for X-ray crystallographic analysis were obtained by layering a CH_2Cl_2 solution with Et_2O. ^{1}H NMR (CD_2Cl_2, 400 MHz): δ 8.06−7.93 (m, 2H, H_{Ph}), 7.78−7.64 (m, 3H, H_{Ar}), 7.10 (s, 2H, H_{Mes}), 4.84 (s, 5H, Cp), 4.10 (s, 3H, NCH_3), 2.40, 2.06 (2 × s, 9H, CH_3-C_{Mes}). $^{13}C\{^1H\}$ NMR (CD_2Cl_2, 101 MHz): δ 211.7 (CO), 153.6 (C_{trz}−Fe), 151.2 (C_{trz}-C_{Ar}), 142.4, 136.3 (2 × C_{Mes}-CH_3), 135.6 (C_{Mes}-N), 132.1, 131.5, 130.0 (3 × C_{Ar}-H), 130.0 (C_{Mes}-H), 127.8 (C_{Ar}-C_{trz}) 86.9 (Cp), 39.3 (NCH_3), 21.4, 18.7 (2 × CH_3-C_{Mes}). IR (CH_2Cl_2, cm^{-1}): 2041, 1994 ν(CO).

*Synthesis of **3c**.* The complex was prepared from **1c** (250 mg; 0.65 mmol), KO*t*Bu (87 mg; 0.78 mmol), and $[CpFe(CO)_2I]$ (177 mg; 0.58 mmol). $AgBF_4$ (152 mg; 0.78 mmol) was added to a CH_2Cl_2 solution of the crude product and the mixture stirred in the dark for 1 h. The solution was collected by filtration over Celite, concentrated to ca. 3 mL, and layered with hexane (15 mL). Single crystals suitable for X-ray crystallographic analysis were obtained in addition to crystallized triazolium salt. The crystals were manually separated to obtain a trace amount of the pure compound for analysis. ^{1}H NMR (CD_2Cl_2, 400 MHz): δ 7.08 (s, 2H, H_{Mes}), 5.11 (s, 5H, Cp), 4.21 (s, 3H, NCH_3), 3.01−2.87 (m, 2H, NCH_2), 2.39 (s, 3H, CH_3-C_{Mes}), 1.87 (s, 6H, CH_3-C_{Mes}), 1.73−1.52 (m, 4H, CH_2), 1.05 (t, J = 7.1 Hz, 3H, CH_3-CH_2). $^{13}C\{^1H\}$ NMR (CD_2Cl_2, 101 MHz): δ 211.7 (CO), 151.5 (C_{trz}-CH_2), 150.9 (C_{trz}-Fe), 142.2, 135.9 (2 × C_{Mes}-CH_3), 135.6 (C_{Mes}-N), 129.9 (C_{Mes}-H), 86.7 (Cp), 37.8 (NCH_3), 31.0 (CH_2), 26.1 (CH_2-C_{trz}), 23.3 (CH_2), 21.4, 17.6 (2 × CH_3-C_{Mes}), 13.9 (CH_3-CH_2). IR (CH_2Cl_2, cm^{-1}): 2041, 1994 ν(CO).

*Synthesis of **4a**.* The complex was prepared from **1a** (100 mg; 0.22 mmol), KO*t*Bu (30 mg; 0.27 mmol), and $[CpFe(CO)_2I]$ (75 mg; 0.25 mmol). The crude product was irradiated for 20 h in CH_2Cl_2 (5 mL). The resulting green solution was concentrated to ∼2 mL and layered with dry hexane. After 24 h, the solution was filtered and evaporated to dryness to yield a dark green solid (37 mg; 28%). Single crystals suitable for X-ray crystallographic analysis were grown from an Et_2O/hexane mixture stored at −20 °C. ^{1}H NMR (CD_2Cl_2, 400 MHz): δ 7.18, 7.14, 7.10, 7.06 (4 × s, 4H, H_{Mes}), 4.07 (s, 5H, Cp), 3.73 (s, 3H, NCH_3), 2.45, 2.42, 2.37, 2.11, 2.04, 1.93 (6 × s, 18H, CH_3-C_{Mes}). $^{13}C\{^1H\}$ NMR (CD_2Cl_2, 101 MHz): δ 221.6 (CO), 176.8 (C_{trz}−Fe), 149.7 (C_{trz}-C_{Mes}), 141.0, 140.9, 140.9, 138.9, 137.6, 136.9, 136.1 (7 × C_{Mes}), 129.9, 129.8, 129.4, 129.1 (4 × C_{Mes}-H), 126.4 (C_{Mes}), 79.8 (Cp), 36.6 (NCH_3), 22.8, 21.5, 21.4, 20.6, 19.3, 18.7 (6 × CH_3-C_{Mes}). IR (CH_2Cl_2, cm^{-1}): 1933 ν(CO). HR-MS (ESI): calcd for $C_{26}H_{30}N_3Fe$ $[M - I - CO]^+$ m/z 440.1784, found m/z 440.1781. Anal. Found (calcd) for $C_{27}H_{30}FeIN_3O \cdot 1/5CH_2Cl_2$ (595.30): C, 53.76 (53.36); H, 5.31 (5.00); N, 6.47 (6.86).

*Synthesis of **4b**.* The complex was prepared from **1b** (220 mg; 0.54 mmol), KO*t*Bu (74 mg; 0.66 mmol), and $[CpFe(CO)_2I]$ (150 mg; 0.49 mmol). The crude product was irradiated for 20 h in CH_2Cl_2 (5 mL). The resulting green solution was concentrated to ∼2 mL and layered with dry hexane. After 24 h, the solution was filtered and evaporated to dryness to yield a dark green solid (129 mg; 48%). Single crystals suitable for X-ray crystallographic analysis were obtained after several days by layering a CH_2Cl_2 solution with hexane. ^{1}H NMR (CD_2Cl_2, 400 MHz): δ 8.26−7.85 (m, 2H, H_{Ar}), 7.74−7.64 (m, 3H, H_{Ar}), 7.09, 7.04 (2 × s, 2H, H_{Mes}), 3.99 (s, 5H, Cp), 3.88 (s, 3H, NCH_3), 2.41, 1.98, 1.82 (3 × s, 9H, CH_3-C_{Mes}). $^{13}C\{^1H\}$ NMR (CD_2Cl_2, 101 MHz): δ 221.8 (CO), 176.9 (C_{trz}−Fe), 150.9 (C_{trz}-C_{Ar}),

DOI: 10.1021/acs.organomet.7b00349
Organometallics XXXX, XXX, XXX−XXX

140.9, 137.7, 137.2, 135.5 (4 × C_{Mes}), 132.1 (C_{Ar}-H), 130.5, 130.5 (2 × C_{Ar}), 129.9 (C_{Mes}-H), 129.2 (C_{Ar}-H), 129.1 (C_{Mes}-H), 80.4 (Cp), 37.6 (NCH_3), 21.4, 19.0, 17.9 (3 × CH_3-C_{Mes}). IR (CH_2Cl_2, cm^{-1}): 1935 ν(CO). HR-MS (ESI): calcd for $C_{23}H_{24}N_3Fe$ $[M - I - CO]^+$ m/z 398.1320, found m/z 398.1339. Anal. Found (calcd) for $C_{24}H_{24}FeIN_3O$ (553.22): C, 51.78 (52.11); H, 3.99 (4.37); N, 7.42 (7.60).

Synthesis of ***4c***. The complex was prepared from **1c** (250 mg; 0.65 mmol), KO*t*Bu (87 mg; 0.78 mmol), and $[CpFe(CO)_2I]$ (177 mg; 0.58 mmol). The crude product was irradiated for 20 h in CH_2Cl_2 (5 mL). The resulting green solution was concentrated to ∼2 mL and layered with dry hexane. After 24 h, the solution was filtered and evaporated to dryness to yield a dark green solid (127 mg; 41%). Single crystals suitable for X-ray crystallographic analysis were obtained after several days by layering a CH_2Cl_2 solution with hexane. ^{1}H NMR (CD_2Cl_2, 400 MHz): δ 7.03, 7.01 (2 × s, 2H, H_{Mes}), 4.38 (s, 5H, Cp), 4.08 (s, 3H, NCH_3), 3.90 (ddd, 1H, J = 15.0, 12.7, 4.7 Hz), 3.09 (ddd, 1H, J = 15.0, 12.1, 4.7 Hz), 2.40 (s, 3H, CH_3-C_{Mes}), 2.00−1.88, 1.88−1.78 (2 × m, 2H, CH_2-C_{trz}), 1.78−1.67 (m, 2H, CH_2), 1.77, 1.74 (2 × s, 6H, CH_3-C_{Mes}), 1.14 (t, J = 7.3 Hz, CH_3-CH_2). ^{13}C{^{1}H} NMR (CD_2Cl_2, 101 MHz): δ 222.5 (CO), 173.7 (C_{trz}-Fe), 151.7 (C_{trz}-CH_2), 140.5, 138.1, 137.3, 134.8 (4 × C_{Mes}), 129.7, 128.9 (2 × C_{Mes}-H), 80.1 (Cp), 37.0 (NCH_3), 31.5 (CH_2), 28.5 (CH_2-C_{trz}), 23.7 (CH_2), 21.4, 18.4, 17.6 (3 × CH_3-C_{Mes}), 14.2 (CH_3-CH_2). IR (CH_2Cl_2, cm^{-1}): 1935 ν(CO). HR-MS (ESI): calcd for $C_{21}H_{28}N_3Fe$ $[M - I - CO]^+$ m/z 378.1627, found m/z 378.1618. Anal. Found (calcd) for $C_{22}H_{28}FeIN_3O$ (533.23): C, 49.97 (49.55); H, 5.26 (5.29); N, 7.43 (7.88).

Synthesis of ***4d***. The complex was prepared from **1d** (150 mg; 0.39 mmol), KO*t*Bu (52 mg; 0.46 mmol), and $[CpFe(CO)_2I]$ (101 mg; 0.33 mmol). After the mixture was stirred for 16 h, the solution was was evaporated to dryness, extracted with CH_2Cl_2 (5 mL), and irradiated for 20 h. The resulting green solution was concentrated to ∼2 mL and layered with dry hexane. After 24 h, the solution was filtered and evaporated to dryness to yield a dark green solid (125 mg; 60%). Single crystals suitable for X-ray crystallographic analysis were obtained after several days by layering a CH_2Cl_2 solution with hexane. ^{1}H NMR (CD_2Cl_2, 300 MHz): δ 7.03, 7.01 (2 × s, 2H, H_{Mes}), 5.27−5.15 (m, 2H, NCH_2) 4.36 (s, 5H, Cp), 3.59 (s, 3H, NCH_3), 2.38 (s, 3H, CH_3-C_{Mes}), 2.27−2.12 (m, 2H, CH_2), 1.84, 1.82 (2 × s, 6H, CH_3-C_{Mes}), 1.74−1.56 (m, 2H, CH_2), 1.11 (t, J = 7.4 Hz, 3H, CH_3-CH_2). ^{13}C{^{1}H} NMR (CD_2Cl_2, 101 MHz): δ 222.8 (CO), 170.1 (C_{trz}-Fe), 147.3 (C_{trz}-^{n}Bu), 140.9, 140.5, 138.4 (3 × C_{Mes}-CH_3), 129.2, 128.7 (2 × C_{Mes}-H), 125.7 (C_{Mes}-C_{trz}), 80.0 (Cp), 56.1 (NCH_2), 36.3 (NCH_3), 32.9 (CH_2), 21.5 (CH_3-C_{Mes}), 20.8 (CH_2), 20.4, 20.1 (2 × CH_3-C_{Mes}), 14.2 (CH_3-CH_2). IR (CH_2Cl_2, cm^{-1}): 1937 ν(CO). HR-MS (ESI): calcd for $C_{21}H_{28}N_3Fe$ $[M - I - CO]^+$ m/z 378.1627, found m/z 378.1615. Anal. Found (calcd) for $C_{22}H_{28}FeIN_3O$ (533.23): C, 49.58 (49.55); H, 5.68 (5.29); N, 7.51 (7.88).

Synthesis of ***5***. The complex was prepared from **1e** (93 mg; 0.22 mmol), KO*t*Bu (29 mg; 0.26 mmol), and $[CpFe(CO)_2I]$ (59 mg; 0.20 mmol). The crude product was redissolved in dry CH_2Cl_2 and layered with Et_2O to yield an analytically pure sample (41 mg; 34%). The filtrate and washings were evaporated to dryness, dissolved in CH_2Cl_2, and layered with Et_2O to give another batch of orange crystals (35 mg; total yield 76 mg, 69%). Slow diffusion of hexane into a CH_2Cl_2 solution of the compound yielded rectangular orange single crystals suitable for X-ray diffraction. ^{1}H NMR (CD_2Cl_2, 300 MHz): δ 8.76 (d, J = 5.4 Hz, 1H, H_{py}), 8.30 (d, J = 8.0 Hz, 1H, H_{py}), 8.12−8.01 (m, 1H, H_{py}), 7.33−7.23 (m, 1H, H_{py}), 7.13, 7.10 (2 × s, 2H, H_{Mes}), 4.72 (s, 3H, NCH_3), 4.48 (s, 5H, Cp), 2.40, 2.21, 2.15 (3 × s, 9H, CH_3-C_{Mes}). ^{13}C{^{1}H} NMR (CD_2Cl_2, 101 MHz): δ 217.5 (CO), 183.3 (C_{trz}-Fe), 158.8 (C_{pyr}-H), 152.1 (C_{pyr}), 146.6 (C_{trz}-C_{pyr}), 141.8 (C_{Mes}), 139.2 (C_{pyr}-H), 135.2, 135.2, 134.6 (3 × C_{Mes}), 130.1, 129.8 (2 × C_{Mes}-H), 124.0, 122.7 (2 × C_{pyr}-H), 81.8 (Cp), 40.7 (NCH_3), 21.3, 18.1, 17.9 (3 × CH_3-C_{Mes}). IR (CH_2Cl_2, cm^{-1}): 1971 ν(CO). HR-MS (ESI): calcd for $C_{23}H_{23}N_4OFe$ $[M - I]^+$ m/z 427.1216, found m/z 427.1221. Anal. Found (calcd) for $C_{23}H_{23}FeIN_4O$ (554.20): C, 49.82 (49.85); H, 3.98 (4.18); N, 9.97 (10.11).

Synthesis of 6. Complex **5** (50 mg; 0.090 mmol) and silver tetrafluoroborate (21 mg; 0.11 mmol) were stirred in dry CH_2Cl_2 (5 mL) in the dark for 1 h. The orange solution was collected by filtration over Celite and layered with dry Et_2O. The resulting orange microcrystals were collected by filtration and dried in vacuo (24 mg; 53%). ^{1}H NMR (CD_2Cl_2, 400 MHz): δ 8.74 (d, J = 5.5 Hz, 1H, H_{py}), 8.12−7.98 (m, 2H, H_{py}), 7.32−7.22 (m, 1H, H_{py}), 7.14, 7.10 (2 × s, 2H, H_{Mes}), 4.61 (s, 3H, NCH_3), 4.46 (s, 5H, Cp), 2.40, 2.20, 2.15 (3 × s, 9H, CH_3-C_{Mes}). ^{13}C{^{1}H} NMR (CD_2Cl_2, 101 MHz): δ 217.5 (CO), 183.5 (C_{trz}-Fe), 158.7 (C_{pyr}-H), 152.2 (C_{pyr}), 146.5 (C_{trz}-C_{pyr}), 141.9 (C_{Mes}), 139.1 (C_{pyr}-H), 135.3, 135.2, 134.7 (3 × C_{Mes}), 130.1, 129.9 (2 × C_{Mes}-H), 124.0, 122.0 (2 × C_{pyr}-H), 81.8 (Cp), 39.5 (NCH_3), 21.4, 17.9, 17.8 (3 × CH_3-C_{Mes}). HR-MS (ESI): calcd for $C_{23}H_{23}N_4OFe$ $[M]^+$ m/z 427.1216, found m/z 427.1207. IR (CH_2Cl_2, cm^{-1}): 1971 ν(CO). Anal. Found (calcd) for $C_{23}H_{23}BF_4FeN_4O$ (514.10): C, 53.62 (53.73); H, 4.53 (4.51); N, 10.60 (10.90).

General Procedure for Hydrosilylation Catalysis. A solution of the relevant aldehyde (0.5 mmol), phenylsilane (74 μL; 0.6 mmol), and hexamethylbenzene (8.1 mg; 0.05 mmol; internal standard in DCE) or 1,3,5-trimethoxybenzene (42 mg; 0.25 mmol; internal standard in THF) in 1,2-dichloroethane or THF (2.5 mL) was equilibrated to 60 °C for 10 min under an N_2 atmosphere. The catalyst was added as a solid (5 μmol), and aliquots were taken at specific times, diluted with $CDCl_3$, and analyzed by ^{1}H NMR spectroscopy.

Crystallographic Details. All measurements were made on an Oxford Diffraction SuperNova area-detector diffractometer using mirror optics monochromated Mo Kα radiation (λ = 0.71073 Å) and Al filtering.[42] Data reduction was performed using the CrysAlisPro program. The intensities were corrected for Lorentz and polarization effects, and a numerical absorption correction based on Gaussian integration over a multifaceted crystal model was applied. Data collection and refinement parameters are presented in the Supporting Information. The structures were solved by direct methods using SHELXT,[43] which revealed the positions of all non-hydrogen atoms of the title compounds. The non-hydrogen atoms were refined anisotropically. All nonacidic H atoms were placed in geometrically calculated positions and refined using a riding model where each H atom was assigned a fixed isotropic displacement parameter with a value equal to 1.2 times the U_{eq} value of its parent atom (1.5 times the U_{eq} value for the methyl groups). Refinement of the structures was carried out on F^2 using full-matrix least-squares procedures, which minimized the function $\sum w(F_o^2 - F_c^2)^2$. The weighting scheme was based on counting statistics and included a factor to downweight the intense reflections. All calculations were performed using the SHELXL-2014/7[44] program. Further crystallographic details are compiled in Tables S1 and S2 in the Supporting Information. Crystallographic data for the structures of all compounds reported in this paper have been deposited with the Cambridge Crystallographic Data Centre (CCDC) as supplementary publication numbers 1546613 (**2a**), 1546614 (**2b**), 1546615 (**3c**), 1546616 (**4a**), 1546617 (**4b**), and 1546618 (**5**).

■ ASSOCIATED CONTENT

Supporting Information

The Supporting Information is available free of charge on the ACS Publications website at DOI: 10.1021/acs.organomet.7b00349.

Crystallographic details for all structures, NMR spectra, cyclic voltammograms, and catalytic details (PDF)

Accession Codes

CCDC 1546613−1546618 contain the supplementary crystallographic data for this paper. These data can be obtained free of charge via www.ccdc.cam.ac.uk/data_request/cif, or by emailing data_request@ccdc.cam.ac.uk, or by contacting The Cambridge Crystallographic Data Centre, 12 Union Road, Cambridge CB2 1EZ, UK; fax: +44 1223 336033.

DOI: 10.1021/acs.organomet.7b00349
Organometallics XXXX, XXX, XXX−XXX

AUTHOR INFORMATION

Corresponding Author

*E-mail for M.A.: martin.albrecht@dcb.unibe.ch.

ORCID

Martin Albrecht: 0000-0001-7403-2329

Notes

The authors declare no competing financial interest.

ACKNOWLEDGMENTS

We acknowledge generous financial support from the European Research Council (CoG 615653) and from the Swiss National Science Foundation (200021_162868, R'equip projects 206021_128724 and 206021_170755). We thank the group of Chemical Crystallography of the University of Bern for X-ray analyses.

REFERENCES

(1) (a) Bolm, C.; Legros, J.; Le Paih, J.; Zani, L. *Chem. Rev.* **2004**, *104*, 6217−6254. (b) Bauer, I.; Knölker, H.-J. *Chem. Rev.* **2015**, *115*, 3170−3387. (c) *Iron Catalysis in Organic Chemistry*; Plietker, B., Ed.; Wiley-VCH: Weinheim, Germany, 2008.

(2) For reviews see: (a) Gaillard, S.; Renaud, J.-L. *ChemSusChem* **2008**, *1*, 505−509. (b) Morris, R. H. *Chem. Soc. Rev.* **2009**, *38*, 2282−2291. (c) Zhang, M.; Zhang, A. *Appl. Organomet. Chem.* **2010**, *24*, 751−757. (d) Enthaler, S.; Junge, K.; Beller, M. Reduction of Unsaturated Compounds with Homogeneous Iron Catalysts. In *Iron Catalysis in Organic Chemistry*; Wiley-VCH: Weinheim, Germany, 2008; pp 125−145. (e) Le Bailly, B. A. F.; Thomas, S. P. *RSC Adv.* **2011**, *1*, 1435−1445. (f) Junge, K.; Schroder, K.; Beller, M. *Chem. Commun.* **2011**, *47*, 4849−4859. (g) Chirik, P. J. Modern Alchemy: Replacing Precious Metals with Iron in Catalytic Alkene and Carbonyl Hydrogenation Reactions. In *Catalysis without Precious Metals*; Wiley-VCH: Weinheim, Germany, 2010; pp 83−110. For selected highlights see: (h) Bart, S. C.; Lobkovsky, E.; Chirik, P. J. *J. Am. Chem. Soc.* **2004**, *126*, 13794−13807. (i) Casey, C. P.; Guan, H. *J. Am. Chem. Soc.* **2007**, *129*, 5816−5817. (j) Langer, R.; Leitus, G.; Ben-David, Y.; Milstein, D. *Angew. Chem., Int. Ed.* **2011**, *50*, 2120−2124. (k) Ziebart, C.; Federsel, C.; Anbarasan, P.; Jackstell, R.; Baumann, W.; Spannenberg, A.; Beller, M. *J. Am. Chem. Soc.* **2012**, *134*, 20701−20704. (l) Zuo, W.; Lough, A. J.; Li, Y. F.; Morris, R. H. *Science* **2013**, *342*, 1080−1083.

(3) (a) *N-Heterocyclic Carbenes: From Laboratory Curiosities to Efficient Synthetic Tools*; Diez-Gonzalez, S., Ed.; The Royal Society of Chemistry: Cambridge, U.K., 2011; RSC Catalysis Series *27*. (b) Cavallo, L.; Cazin, C. S. J., N-Heterocyclic Carbenes: An Introductory Overview. In *N-Heterocyclic Carbenes in Transition Metal Catalysis and Organocatalysis*; Cazin, C. S. J., Ed.; Springer: Dordrecht, The Netherlands, 2011; pp 1−22. (c) Melaimi, M.; Soleilhavoup, M.; Bertrand, G. *Angew. Chem., Int. Ed.* **2010**, *49*, 8810−8849. (d) Díez-González, S.; Marion, N.; Nolan, S. P. *Chem. Rev.* **2009**, *109*, 3612−3676. (e) Liddle, S. T.; Edworthy, I. S.; Arnold, P. L. *Chem. Soc. Rev.* **2007**, *36*, 1732−1744. (f) Hopkinson, M. N.; Richter, C.; Schedler, M.; Glorius, F. *Nature* **2014**, *510*, 485−496. (g) Poyatos, M.; Mata, J. A.; Peris, E. *Chem. Rev.* **2009**, *109*, 3677−3707.

(4) Riener, K.; Haslinger, S.; Raba, A.; Högerl, M. P.; Cokoja, M.; Herrmann, W. A.; Kühn, F. E. *Chem. Rev.* **2014**, *114*, 5215−5272.

(5) Kandepi, V. V. K. M.; Cardoso, J. M. S.; Peris, E.; Royo, B. *Organometallics* **2010**, *29*, 2777−2782.

(6) (a) Demir, S.; Gökçe, Y.; Kaloğlu, N.; Sortais, J.-B.; Darcel, C.; Özdemir, İ. *Appl. Organomet. Chem.* **2013**, *27*, 459−464. (b) Blom, B.; Tan, G.; Enthaler, S.; Inoue, S.; Epping, J. D.; Driess, M. *J. Am. Chem. Soc.* **2013**, *135*, 18108−18120. (c) Buitrago, E.; Zani, L.; Adolfsson, H. *Appl. Organomet. Chem.* **2011**, *25*, 748−752. (d) Jiang, F.; Bézier, D.; Sortais, J.-B.; Darcel, C. *Adv. Synth. Catal.* **2011**, *353*, 239−244. (e) Lopes, R.; Cardoso, J. M. S.; Postigo, L.; Royo, B. *Catal. Lett.* **2013**, *143*, 1061−1066. (f) Warratz, S.; Postigo, L.; Royo, B. *Organometallics* **2013**, *32*, 893−897.

(7) Bézier, D.; Venkanna, G. T.; Sortais, J.-B.; Darcel, C. *ChemCatChem* **2011**, *3*, 1747−1750.

(8) (a) Castro, L. C. M.; Sortais, J.-B.; Darcel, C. *Chem. Commun.* **2012**, *48*, 151−153. (b) Bhunia, M.; Hota, P. K.; Vijaykumar, G.; Adhikari, D.; Mandal, S. K. *Organometallics* **2016**, *35*, 2930−2937.

(9) Cardoso, J. M. S.; Royo, B. *Chem. Commun.* **2012**, *48*, 4944−4946.

(10) (a) Iglesias, M.; Fernández-Alvarez, F. J.; Oro, L. A. *ChemCatChem* **2014**, *6*, 2486−2489. (b) Riener, K.; Högerl, M. P.; Gigler, P.; Kühn, F. E. *ACS Catal.* **2012**, *2*, 613−621.

(11) Mathew, P.; Neels, A.; Albrecht, M. *J. Am. Chem. Soc.* **2008**, *130*, 13534−13535.

(12) (a) Himo, F.; Lovell, T.; Hilgraf, R.; Rostovtsev, V. V.; Noodleman, L.; Sharpless, K. B.; Fokin, V. V. *J. Am. Chem. Soc.* **2005**, *127*, 210−216. (b) Rostovtsev, V. V.; Green, L. G.; Fokin, V. V.; Sharpless, K. B. *Angew. Chem., Int. Ed.* **2002**, *41*, 2596−2599.

(13) (a) Crowley, J. D.; Lee, A.-L.; Kilpin, K. J. *Aust. J. Chem.* **2011**, *64*, 1118−1132. (b) Albrecht, M. *Chem. Commun.* **2008**, 3601−3610. (c) Chianese, A. R.; Kovacevic, A.; Zeglis, B. M.; Faller, J. W.; Crabtree, R. H. *Organometallics* **2004**, *23*, 2461−2468. (d) Terashima, T.; Inomata, S.; Ogata, K.; Fukuzawa, S.-i. *Eur. J. Inorg. Chem.* **2012**, *2012*, 1387−1393. (e) Yuan, D.; Huynh, H. V. *Organometallics* **2012**, *31*, 405−412. (f) Donnelly, K. F.; Petronilho, A.; Albrecht, M. *Chem. Commun.* **2013**, *49*, 1145−1159.

(14) (a) Bouffard, J.; Keitz, B. K.; Tonner, R.; Guisado-Barrios, G.; Frenking, G.; Grubbs, R. H.; Bertrand, G. *Organometallics* **2011**, *30*, 2617−2627. (b) Cai, J.; Yang, X.; Arumugam, K.; Bielawski, C. W.; Sessler, J. L. *Organometallics* **2011**, *30*, 5033−5037. (c) Keitz, B. K.; Bouffard, J.; Bertrand, G.; Grubbs, R. H. *J. Am. Chem. Soc.* **2011**, *133*, 8498−8501.

(15) (a) Mendoza-Espinosa, D.; González-Olvera, R.; Negrón-Silva, G. E.; Angeles-Beltrán, D.; Suárez-Castillo, O. R.; Álvarez-Hernández, A.; Santillan, R. *Organometallics* **2015**, *34*, 4529−4542. (b) Keske, E. C.; Zenkina, O. V.; Wang, R.; Crudden, C. M. *Organometallics* **2012**, *31*, 6215−6221. (c) Canseco-Gonzalez, D.; Gniewek, A.; Szulmanowicz, M.; Müller-Bunz, H.; Trzeciak, A. M.; Albrecht, M. *Chem. - Eur. J.* **2012**, *18*, 6055−6062. (d) Wei, Y.; Petronilho, A.; Mueller-Bunz, H.; Albrecht, M. *Organometallics* **2014**, *33*, 5834−5844. (e) Karthikeyan, T.; Sankararaman, S. *Tetrahedron Lett.* **2009**, *50*, 5834−5837.

(16) (a) Petronilho, A.; Llobet, A.; Albrecht, M. *Inorg. Chem.* **2014**, *53*, 12896−12901. (b) Lalrempuia, R.; McDaniel, N. D.; Müller-Bunz, H.; Bernhard, S.; Albrecht, M. *Angew. Chem., Int. Ed.* **2010**, *49*, 9765−9768. (c) Bernet, L.; Lalrempuia, R.; Ghattas, W.; Mueller-Bunz, H.; Vigara, L.; Llobet, A.; Albrecht, M. *Chem. Commun.* **2011**, *47*, 8058−8060. (d) Petronilho, A.; Rahman, M.; Woods, J. A.; Al-Sayyed, H.; Muller-Bunz, H.; Don MacElroy, J. M.; Bernhard, S.; Albrecht, M. *Dalton Trans.* **2012**, *41*, 13074−13080. (e) Woods, J. A.; Lalrempuia, R.; Petronilho, A.; McDaniel, N. D.; Muller-Bunz, H.; Albrecht, M.; Bernhard, S. *Energy Environ. Sci.* **2014**, *7*, 2316−2328. (f) Corbucci, I.; Petronilho, A.; Müller-Bunz, H.; Rocchigiani, L.; Albrecht, M.; Macchioni, A. *ACS Catal.* **2015**, *5*, 2714−2718.

(17) (a) Valencia, M.; Muller-Bunz, H.; Gossage, R. A.; Albrecht, M. *Chem. Commun.* **2016**, *52*, 3344−3347. (b) Sabater, S.; Müller-Bunz, H.; Albrecht, M. *Organometallics* **2016**, *35*, 2256−2266. (c) Bagh, B.; McKinty, A. M.; Lough, A. J.; Stephan, D. W. *Dalton Trans.* **2014**, *43*, 12842−12850. (d) Canseco-Gonzalez, D.; Albrecht, M. *Dalton Trans.* **2013**, *42*, 7424−7432. (e) Delgado-Rebollo, M.; Canseco-Gonzalez, D.; Hollering, M.; Mueller-Bunz, H.; Albrecht, M. *Dalton Trans.* **2014**, *43*, 4462−4473.

(18) (a) Iwasaki, H.; Yamada, Y.; Ishikawa, R.; Koga, Y.; Matsubara, K. *Eur. J. Org. Chem.* **2016**, *2016*, 1651−1654. (b) Liu, Y.; Kjær, K. S.; Fredin, L. A.; Chábera, P.; Harlang, T.; Canton, S. E.; Lidin, S.; Zhang, J.; Lomoth, R.; Bergquist, K.-E.; Persson, P.; Wärnmark, K.; Sundström, V. *Chem. - Eur. J.* **2015**, *21*, 3628−3639. (c) Nakamura, T.; Terashima, T.; Ogata, K.; Fukuzawa, S.-i. *Org. Lett.* **2011**, *13*, 620−623. (d) Hohloch, S.; Duecker, F.; van der Meer, M.; Sarkar, B. *Molecules* **2015**, *20*, 7379.

DOI: 10.1021/acs.organomet.7b00349
Organometallics XXXX, XXX, XXX−XXX

(19) Wei, Y.; Liu, S.-X.; Müller-Bunz, H.; Albrecht, M. *ACS Catal.* **2016**, *6*, 8192−8200.
(20) (a) Guisado-Barrios, G.; Bouffard, J.; Donnadieu, B.; Bertrand, G. *Angew. Chem., Int. Ed.* **2010**, *49*, 4759−4762. (b) Buchgraber, P.; Toupet, L.; Guerchais, V. *Organometallics* **2003**, *22*, 5144−5147. (c) Mercs, L.; Labat, G.; Neels, A.; Ehlers, A.; Albrecht, M. *Organometallics* **2006**, *25*, 5648−5656.
(21) (a) Valyaev, D. A.; Brousses, R.; Lugan, N.; Fernández, I.; Sierra, M. A. *Chem. - Eur. J.* **2011**, *17*, 6602−6605. (b) Fernández, I.; Lugan, N.; Lavigne, G. *Organometallics* **2012**, *31*, 1155−1160.
(22) Because of the presence of an induction time, the more common notion of TOF_{25} or TOF_{50} (i.e., turnover frequency at 25 or 50% conversion) is not very meaningful for characterizing the efficiency of the catalyst. We therefore report TOF_{max}: i.e., the highest recorded turnover frequency during substrate conversion.
(23) Attempts to monitor the complex during this induction time were unsuccessful. React-IR measurements under catalytic conditions did not reveal any changes, presumably because the concentration of the Fe complex is too low. Increasing the concentration of the Fe complex for NMR spectroscopic monitoring accelerated the reaction rate substantially and abolished the induction time completely.
(24) Hansch, C.; Leo, A.; Taft, R. W. *Chem. Rev.* **1991**, *91*, 165−195.
(25) We observe the same acceleration of conversion of 4-bromoacetophenone in the presence of 4-bromobenzaldehyde in THF solvent (see Figure S25 in the Supporting Information). This supports the model that the catalytically active species is formed faster in the presence of the aldehyde substrate and that the activation is not related to the solvent.
(26) (a) Lavallo, V.; Grubbs, R. H. *Science* **2009**, *326*, 559−562. (b) Lavallo, V.; El-Batta, A.; Bertrand, G.; Grubbs, R. H. *Angew. Chem., Int. Ed.* **2011**, *50*, 268−271. (c) Layfield, R. A.; McDouall, J. J. W.; Scheer, M.; Schwarzmaier, C.; Tuna, F. *Chem. Commun.* **2011**, *47*, 10623−10625. (d) Ingleson, M. J.; Layfield, R. A. *Chem. Commun.* **2012**, *48*, 3579−3589. (e) Zlatogorsky, S.; Ingleson, M. J. *Dalton Trans.* **2012**, *41*, 2685−2693. (f) Day, B. M.; Pugh, T.; Hendriks, D.; Guerra, C. F.; Evans, D. J.; Bickelhaupt, F. M.; Layfield, R. A. *J. Am. Chem. Soc.* **2013**, *135*, 13338−13341. (g) Dunsford, J. J.; Cade, I. A.; Fillman, K. L.; Neidig, M. L.; Ingleson, M. J. *Organometallics* **2014**, *33*, 370−377. (h) Musgrave, R. A.; Turbervill, R. S. P.; Irwin, M.; Herchel, R.; Goicoechea, J. M. *Dalton Trans.* **2014**, *43*, 4335−4344. (i) Haslinger, S.; Kück, J. W.; Anneser, M. R.; Cokoja, M.; Pöthig, A.; Kühn, F. E. *Chem. - Eur. J.* **2015**, *21*, 17860−17869.
(27) (a) Marion, N.; Díez-González, S.; Nolan, S. P. *Angew. Chem.* **2007**, *119*, 3046−3058. (b) Marion, N.; Díez-González, S.; Nolan, S. P. *Angew. Chem., Int. Ed.* **2007**, *46*, 2988−3000. (c) Riduan, S. N.; Zhang, Y.; Ying, J. Y. *Angew. Chem., Int. Ed.* **2009**, *48*, 3322−3325. (d) Tan, M.; Zhang, Y.; Ying, J. Y. *Adv. Synth. Catal.* **2009**, *351*, 1390−1394. (e) Huang, F.; Lu, G.; Zhao, L.; Li, H.; Wang, Z.-X. *J. Am. Chem. Soc.* **2010**, *132*, 12388−12396. (f) Revunova, K.; Nikonov, G. I. *Dalton. Trans.* **2015**, *44*, 840−866.
(28) The ^{1}H and ^{13}C NMR resonances we recorded differed from reported values.[28a] However, we prepared the compound by three independent methods (quenching of the free carbene with S_8 and exposing the AgX(IMes) and [CpFe(IMes)(CO)I] complexes to S_8 for 2 h at 60 °C), yielding identical NMR spectra. ^{1}H NMR (C_6D_6, 400 MHz): δ 6.77 (s, 4H, H_{Mes}), 5.92 (s, 2H, H_{Imid}), 2.14, 2.11 (2*s*, 18H, CH_3-C_{Mes}). $^{13}C\{^{1}H\}$ NMR (C_6D_6; 101 MHz): δ 165.1 (C═S), 138.9 (C_{Mes}), 136.17 (C_{Mes}), 134.7 (C_{Mes}), 129.4 (C_{Mes}-H), 117.4 (C_{Imid}-H), 21.1, 18.1 (2 × CH_3-C_{Mes}). Furthermore, our assignment of the C═S carbon resonance agrees with that observed by Arduengo for this compound.[28b]b HR-MS (ESI) confirmed the chemical formula $C_{21}H_{25}N_2S$ $[M + H]^+$ (calculated 337.1725; found 337.1733). (a) Ramnial, T.; Taylor, S. A.; Bender, M. L.; Gorodetsky, B.; Lee, P. T. K.; Dickie, D. A.; McCollum, B. M.; Pye, C. C.; Walsby, C. J.; Clyburne, J. A. C. *J. Org. Chem.* **2008**, *73*, 801−812. (b) Arduengo, A. J.; Calabrese, J. C.; Cowley, A. H.; Dias, H. V. R.; Goerlich, J. R.; Marshall, W. J.; Riegel, B. *Inorg. Chem.* **1997**, *36*, 2151−2158.
(29) Following purification of the reaction mixture after 10 min by diluting with pentane and filtration through Celite, significant conversion to the thiourea product (thiourea/complex **7**, 4/1) occurred. The relative integration of the thiourea product vs an internal standard (trimethoxybenzene) confirmed essentially quantitative conversion. Since this product was not detected in the intial reaction mixture, we speculate that the Fe−C bond is sensitive to these manipulations. For instance, filtration through slightly acidic Celite may induce Fe−C bond cleavage and facilitate thione formation.
(30) (a) Tran, B. L.; Pink, M.; Mindiola, D. J. *Organometallics* **2009**, *28*, 2234−2243. (b) Chakraborty, S.; Krause, J. A.; Guan, H. *Organometallics* **2009**, *28*, 582−586. (c) Xue, B.; Sun, H.; Li, X. *RSC Adv.* **2015**, *5*, 52000−52006. (d) Bleith, T.; Gade, L. H. *J. Am. Chem. Soc.* **2016**, *138*, 4972−4983.
(31) Fischer, H. *Chem. Rev.* **2001**, *101*, 3581−3610.
(32) Bagh, B.; Stephan, D. W. *Dalton Trans.* **2014**, *43*, 15638−15645.
(33) (a) Muller, N.; Mulliken, R. S. *J. Am. Chem. Soc.* **1958**, *80*, 3489−3497. (b) Henry, D. J.; Parkinson, C. J.; Mayer, P. M.; Radom, L. *J. Phys. Chem. A* **2001**, *105*, 6750−6756. (c) Menon, A. S.; Henry, D. J.; Bally, T.; Radom, L. *Org. Biomol. Chem.* **2011**, *9*, 3636−3657.
(34) Fürstner, A. *ACS Cent. Sci.* **2016**, *2*, 778−789.
(35) (a) Bedford, R. B.; Bruce, D. W.; Frost, R. M.; Hird, M. *Chem. Commun.* **2005**, 4161−4163. (b) Noda, D.; Sunada, Y. *J. Am. Chem. Soc.* **2009**, *131*, 6078−6079. (c) Hatakeyama, T.; et al. *Chem. Lett.* **2011**, *40*, 1030−1032. (d) Hatakeyama, T.; Hashimoto, T.; Kathriarachchi, K. K. A. D. S.; Zenmyo, T.; Seike, H.; Nakamura, M. *Angew. Chem., Int. Ed.* **2012**, *51*, 8834−8837.
(36) Enholm, E. J.; Jia, Z. J. *J. Org. Chem.* **1997**, *62*, 9159−9164.
(37) Tanner, D. D.; Chen, J. J.; Luelo, C.; Peters, P. M. *J. Am. Chem. Soc.* **1992**, *114*, 713−717.
(38) (a) Darmon, J. M.; Stieber, S. C. E.; Sylvester, K. T.; Fernandez, I.; Lobkovsky, E.; Semproni, S. P.; Bill, E.; Wieghardt, K.; DeBeer, S.; Chirik, P. J. *J. Am. Chem. Soc.* **2012**, *134*, 17125−17137. (b) Hoyt, J. M.; Sylvester, K. T.; Semproni, S. P.; Chirik, P. J. *J. Am. Chem. Soc.* **2013**, *135*, 4862−4877. (c) Chirik, P. J. *Acc. Chem. Res.* **2015**, *48*, 1687−1695.
(39) (a) Chalk, A. J.; Harrod, J. F. *J. Am. Chem. Soc.* **1965**, *87*, 16−21. (b) Chan, T. H.; Melnyk, A. *J. Am. Chem. Soc.* **1970**, *92*, 3718−3722. (c) Zheng, G. Z.; Chan, T. H. *Organometallics* **1995**, *14*, 70−79. (d) Glaser, P. B.; Tilley, T. D. *J. Am. Chem. Soc.* **2003**, *125*, 13640−13641. (e) Brunner, H. *Angew. Chem., Int. Ed.* **2004**, *43*, 2749−2750. (f) Chaulagain, M. R.; Mahandru, G. M.; Montgomery, J. *Tetrahedron* **2006**, *62*, 7560−7566. (g) Vergote, T.; Gathy, T.; Nahra, F.; Riant, O.; Peeters, D.; Leyssens, T. *Theor. Chem. Acc.* **2012**, *131*, 1253.
(40) (a) Wiese, S.; Aguila, M. J. B.; Kogut, E.; Warren, T. H. *Organometallics* **2013**, *32*, 2300−2308. (b) Nakamura, T.; Ogata, K.; Fukuzawa, S.-i. *Chem. Lett.* **2010**, *39*, 920−922. (c) Schweinfurth, D.; Pattacini, R.; Strobel, S.; Sarkar, B. *Dalton Trans.* **2009**, 9291−9297. (d) Khan, S. S.; Liebscher, J. *Synthesis* **2010**, *2010*, 2609−2615.
(41) Connelly, N. G.; Geiger, W. E. *Chem. Rev.* **1996**, *96*, 877−910.
(42) Macchi, P.; Burgi, H.-B.; Chimpri, A. S.; Hauser, J. *J. Appl. Crystallogr.* **2011**, *44*, 763−771.
(43) Sheldrick, G. *Acta Crystallogr., Sect. A: Found. Adv.* **2015**, *71*, 3−8.
(44) Sheldrick, G. M. *Acta Crystallogr., Sect. C: Struct. Chem.* **2015**, *71*, 3−8.

DOI: 10.1021/acs.organomet.7b00349
Organometallics XXXX, XXX, XXX−XXX